Probing the subglass relaxation behavior in model heterocyclic polymer networks by dielectric spectroscopy

V. Yu. Kramarenko,[1] T. A. Ezquerra,[2,*] and V. P. Privalko[3]
[1]*State Polytechnic University, Frunze 21, 61002 Kharkov, Ukraine*
[2]*Instituto de Estructura de la Materia, CSIC, Serrano 119, 28006 Madrid, Spain*
[3]*Institute of Macromolecular Chemistry, National Academy of Sciences of Ukraine, Kharkov Chaussee 48, 02160 Kyiv, Ukraine*
(Received 24 May 2001; published 18 October 2001)

The subglass relaxation (β) in model heterocyclic polymer networks (HPNs) with a controlled ratio of trimerized mono- and diisocyanates was characterized by dielectric spectroscopy in the frequency domain. The β relaxation in the investigated HPNs follows the Arrhenius law with unusually low values of the preexponential factor ($10^{-17}<\tau_{\beta 0}<10^{-15}$ s). However, little influence of the local environment, as characterized by the network density, on the apparent activation energies ΔE_β is observed. This fact, combined with their fairly low absolute values (50.4–58.3 kJ/mol), were considered as typical of a noncooperative relaxation in loosely packed regions of a glassy quasilattice. Both the intensity and dielectric strength of the β relaxation in HPNs increase with increasing apparent network density (i.e., with lower ratios of linear and network structures in the system, L/N). This effect was explained by a model assuming that the total, composition-invariant, free volume available was distributed between densely packed domains comprising linear, two-arm isocyanurate heterocycles (ISHs) and loosely packed, three-arm ISHs, which form continuous, three-dimensional network structures. The experimental data for HPNs confirm Ngai's correlation between the logarithm of the secondary β-relaxation time and the Kohlrausch-Williams-Watts stretching exponent for the primary α relaxation. It is suggested that the absence of conjugated bonds within isocyanurate heterocycles makes them sufficiently flexible to allow for specific conformational transitions, like the ''chair-boat-chair'' transition in the structurally similar cyclohexyl ring.

DOI: 10.1103/PhysRevE.64.051802 PACS number(s): 61.41.+e, 64.70.Pf

I. INTRODUCTION

The glass transition temperature T_g is commonly considered as the physical boundary between the equilibrium liquid state and the nonequilibrium metastable glassy state. In the former there exists an essentially unrestricted translational mobility of relevant units, molecules for ''monomeric'' liquids and chain segments for polymers. In the glassy state mobility is arrested except for oscillations of kinetic units around fixed sites of a disordered quasilattice. The multiplicity of relaxations below T_g [1–3] is experimental evidence for the existence of other kinds of thermal motion in the glassy state of polymers. It seems reasonable to associate the lowermost subglass relaxations with the onset of mobility of the smallest kinetic units (e.g., end-chain or/and side-chain groups) in the loosely packed ''pockets'' of a quasilattice. The uppermost subglass relaxation, usually referred to as the β relaxation, has sometimes been associated with a microheterogeneous structure of glasses consisting in a random distribution of densely packed domains of quasicrystalline order within a loosely packed matrix [4–6], although its nature is still a matter of debate [7–9]. Nevertheless, the current view of the most probable scenario of relaxations in glass-forming liquids implies the bifurcation of a single relaxation in the equilibrium liquid range (i.e., at $T \gg T_g$) into a slow (main or α) and a faster (secondary or β) relaxation on the approach to T_g [6,10–12]. The Arrhenius-like temperature dependence of the relaxation times τ_β follows

$$\tau_\beta = \tau_{\beta 0} \exp(\Delta E_\beta / RT) \tag{1}$$

with a fairly low activation energy ΔE_β, suggesting that the fast process belongs to the category of simple, noncooperative transitions.

In contrast, the non-Arrhenius pattern of the temperature dependence of relaxation times τ_α of the slow process is expressed by the empirical Vogel-Tamman-Fulcher (VTF) equation

$$\tau_\alpha = \tau_{\alpha 0} \exp[B/(T-T_0)], \tag{2}$$

where τ_{a0}, B, and T_0 are characteristic constants. The nonexponential pattern of the relaxation process is expressed by the empirical Kohlrausch-Williams-Watts (KWW) function

$$\phi(t) = \exp[-(t/\tau)^{\beta}_{\mathrm{KWW}}], \tag{3}$$

where the noninteger stretching exponent β_{KWW} serves as a phenomenological measure of the width of the continuous relaxation time spectrum. Both equations are assumed to be ''canonical'' features of complex, cooperative relaxations [13].

Although the β relaxation has been extensively studied for linear polymers, not so much attention has been devoted to polymer networks. Secondary relaxations in epoxyamine polymer networks were studied in detail by Johari and coworkers [14–20] using dielectric spectroscopy (DS). Here, the β relaxation was first thought to have a molecular origin. This was attributed either to the localized motions of moi-

*Email address: imte155@iem.cfmac.csic.es

TABLE I. Selected parameters of the studied systems. L/N ratio of linear to network content; M_c, average molecular weight of chain strands between cross links; P, content of polar NCO groups; T^* temperature at which average relaxation time for the α relaxation equals 10^2 s; β_{KWW}, Kohlrausch-Williams-Watts stretching exponent for the α relaxation [24].

L/N	M_c (g/mol)	P (%)	T^* (K)	β_{KWW}
100/0	$\rightarrow\infty$	42.7	291.6	0.43
75/25	1137.0	44.3	311.9	0.39
60/40	694.5	45.4	322.3	0.37
43/57	473.3	46.6	333.0	0.37
0/100	252.0	50.0	351.3	0.29

eties containing secondary hydroxyls, or to the restricted rotation of fragments adjacent to the oxygen bridges of the diglycidyl ether of bisphenol *A*. The intensity of the β process was expected to correlate with the increasing concentration of secondary hydroxyls in the course of the curing reaction [15,16]. However, the assumption of a quantitative correlation between the concentration of any functional group and the intensity of the β relaxation was later abandoned, in favor of a more general scenario that links this process to the noncooperative motion of chain fragments in loosely packed regions of a glassy quasilattice [19,20]. In many polymer networks the true impact of the chemical network density is obscured by side effects including morphological heterogeneity and strong physical interactions [21], incomplete chemical conversion [22], or anomalous chain flexibility of network strands [23] among others. Some of these side effects can be minimized by controlled preparation of model polymer networks with well defined molecular architecture.

In our previous DS studies of model heterocyclic polymer networks (HPNs) [24] the main issue of concern was the influence of cross-link density on the segmental dynamics in the vicinity of the α relaxation. This study was accomplished through analysis of the VTF and KWW behavior (Table I). In agreement with the coupling model [25,26] it was shown that increasing cross-link density enhances the dynamical constrains of the α relaxation, increasing the degree of intermolecular coupling [24]. The unique feature of these HPNs was a broad variation of network junction concentration, keeping essentially invariant the concentration of dielectrically active dipoles. Thus, the network topology turns out to be the dominant aspect affecting the salient features of the relevant relaxation processes. The aim of this work is to extend the previous study to the subglass relaxations in order to reveal both the influence of the cross-link density on the β relaxation and its origin.

II. EXPERIMENT

The details of preparation of the model polymer networks based on hexamethylene diisocyanate and hexyl isocyanate with different ratios and cure conditions were described elsewhere [24]. By this procedure a regularly cross-linked copolymer is obtained with precise molar fractions of three-arm (cross-linked) and two-arm (linear) segments (Fig. 1). Assuming a full conversion of the reacting groups and formation of a defect-free network structure some relevant structural parameters can be calculated (Table I). Here, L/N refers to the ratio of linear to network structure (Fig. 1), M_c is the average molecular weight of a chain segment enclosed between two cross links, and P is the molar content of NCO groups in the copolymers. An important feature of these systems is an almost invariant concentration of dielectrically active components in spite of the significant topology variation. The complex dielectric permittivity $\varepsilon^*=\varepsilon'-i\varepsilon''$ was measured in the frequency range $10^{-1}<F<10^5$ Hz by using a Standford lock-in amplifier SR830 with a dielectric interface and control temperature unit from Novocontrol.

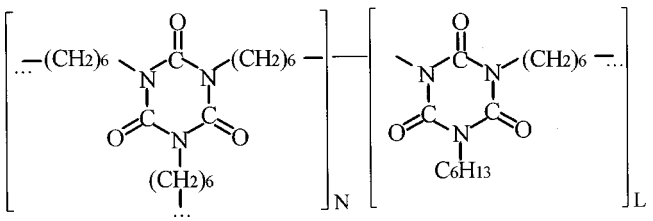

FIG. 1. Generalized chemical scheme of heterocyclic polymer networks.

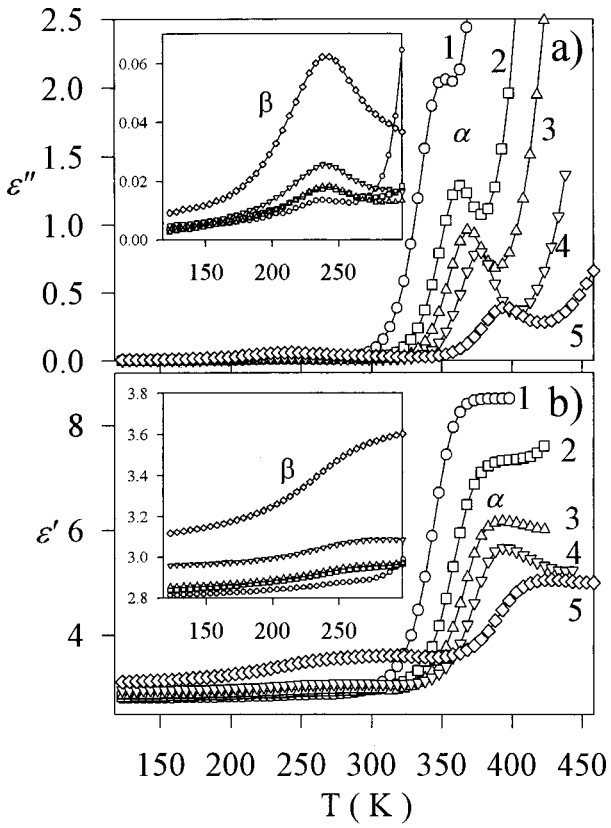

FIG. 2. Dielectric loss (a) and dielectric constant (b) as functions of temperature at 1 kHz for networks with different L/N ratios: line 1, 100/0; line 2, 75/25; line 3, 60/40; line 4, 43/57; line 5, 0/100. Insets show the same data for the region of β relaxation.

TABLE II. Parameters of the secondary relaxation of HPNs. Temperatures T_{max} at the peak maxima of the loss factor. Peak intensities and increments of the storage factor at T_{max}, $\Delta\varepsilon'$.

L/N	$F=10^5$ (Hz)			$F=10^4$ (Hz)			$F=10^3$ (Hz)			$F=10^2$ (Hz)			$F=10^1$ (Hz)			$F=10^0$ (Hz)			$F=10^{-1}$ (Hz)		
	T_{max} (K)	ε'' (units of 10^3)	$\Delta\varepsilon'$ (units of 10^2)	T_{max} (K)	ε'' (units of 10^3)	$\Delta\varepsilon'$ (units of 10^2)	T_{max} (K)	ε'' (units of 10^3)	$\Delta\varepsilon'$ (units of 10^2)	T_{max} (K)	ε'' (units of 10^3)	$\Delta\varepsilon'$ (units of 10^2)	T_{max} (K)	ε'' (units of 10^3)	$\Delta\varepsilon'$ (units of 10^2)	T_{max} (K)	ε'' (units of 10^3)	$\Delta\varepsilon'$ (units of 10^2)	T_{max} (K)	ε'' (units of 10^3)	$\Delta\varepsilon'$ (units of 10^2)
100/0				258	4.1	1.8	248	4.8	1.8	223	4.1	1.7	206	4.4	1.6	188	3.4	1.7	178	3.1	1.9
75/25				263	4.7	4.0	251	7.6	4.2	223	7.8	4.0	205	8.8	4.1	190	8.7	4.0	181	8.0	4.7
60/40	278	5.0	5.8	265	7.4	6.2	251	8.6	6.1	222	9.9	6.5	206	8.8	7.0	193	9.0	6.6	181	8.6	6.5
43/57	278	8.6	6.8	260	12.1	7.4	249	13.6	8.0	223	12.7	9.7	206	12.7	11.2	191	13.7	11.4	181	14.5	12.6
0/100	285	33.8	27.8	260	37.8	32.7	250	42.2	33.4	223	35.2	35.2	207	36.5	36.5	195	36.5	35.1	183	29.1	34.7

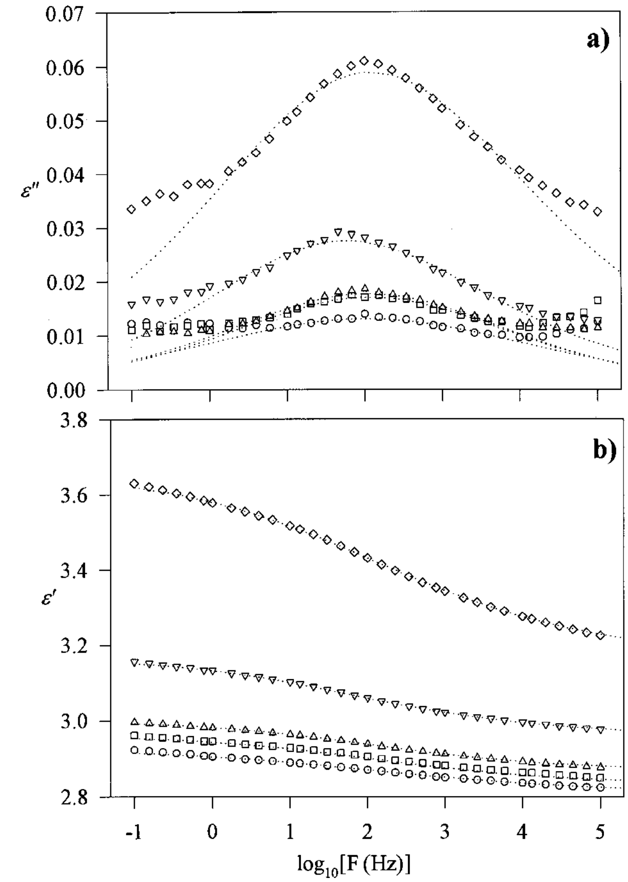

FIG. 3. Dielectric loss ε'' (a) and dielectric constant ε' (b) for HPN networks with varying L/N ratios as functions of frequency at 223 K. The dashed lines represent the best fits to the HN function. Symbols the same as in Fig. 2.

III. RESULTS

As can be seen from the representative isochronal ($F=1$ kHz) temperature dependencies of the imaginary (ε'') and real (ε') parts of the complex dielectric permittivity of HPNs with different L/N ratios (Fig. 2), the most intense α relaxation in the interval 330–400 K shifts to higher temperatures, whereas its intensity decreases, for higher apparent network densities. In contrast, the position of the subglass β relaxation in the interval 170–270 K remains essentially invariant, independent of the L/N ratio. Moreover, its intensity increases with increasing apparent network density. For a more detailed assessment of the features of β relaxation, the temperatures T_{max} at the peak maxima of the loss factor, the corresponding peak intensities ε'', as well as the increments of the storage factor at T_{max},$\Delta\varepsilon'$, were evaluated over the entire interval of measurement frequencies (Table II).

The frequency dependencies of both ε'' and ε' at fixed temperature were fitted (Fig. 3) to the Havriliak-Negami (HN) function, Eq. (4), to derive the broadening parameters b and the dielectric strength $\Delta\varepsilon$ (Table III). It is pertinent to remark at this point that in the majority of cases the best fits were obtained assuming $c=1$ (i.e., the distribution of relaxation times of the β relaxation is described by the symmetric Cole-Cole function). The Havriliak-Negami function reads

TABLE III. Cole-Cole and Havriliak-Negami parameters b and c, and dielectric strength.

	L/N									
	100/0		75/25		60/40		43/57		0/100	
T (K)	b	$\Delta\varepsilon$	b	$\Delta\varepsilon$	b/c[a]	$\Delta\varepsilon$	b/c[a]	$\Delta\varepsilon$	b/c[a]	$\Delta\varepsilon$
208			0.303	0.131	0.408/ 0.673	0.126	0.425/ 0.724	0.185	0.540/ 0.257	0.482
213	0.327	0.101	0.324	0.123	0.351	0.127	0.392	0.188	0.440/0.363	0.500
218	0.287	0.115	0.316	0.126	0.340	0.130	0.388	0.188	0.363/ 0.548	0.500
223	0.281	0.117	0.332	0.120	0.332	0.133	0.361	0.209	0.312/ 0.846	0.498
228	0.321	0.104	0.338	0.118	0.346	0.129	0.311	0.216	0.290	0.512
233	0.303	0.110	0.345	0.116	0.353	0.126	0.286	0.229	0.279	0.536
238	0.312	0.107	0.367	0.111	0.339	0.133	0.252	0.252	0.265	0.571

[a]For samples with higher cross-link densities and/or at relatively low temperatures the best fit was obtained with the Havriliak-Negami function with $c \neq 1$.

$$\varepsilon(\omega)-\varepsilon_\infty=\frac{(\varepsilon_0-\varepsilon_\infty)}{[1+(i\omega\tau)^b]^c} \tag{4}$$

where $\omega=2\pi F$, ε_0 and ε_∞ are the relaxed ($\omega=0$) and unrelaxed ($\omega=\infty$) dielectric constant values, τ is the central relaxation time of the relaxation time distribution function, and b and c are shape parameters that describe the symmetric and asymmetric broadening of the relaxation time distribution function, respectively [27].

IV. DISCUSSION

A. Activation energy of the β relaxation

Figure 4 shows the relaxation map for both the α and β processes. The values corresponding to the α relaxation, described in an earlier publication [24], are represented for completeness. In the region of β relaxation it is seen from the Arrhenius $\log_{10}\tau_{\max}$ vs $f(1/T)$ plots [where $\tau_{\max}=1/(2\pi F_{\max})$, and $F_{\max}$ is the frequency at the ε'' maximum] that the data for all HPNs studied fall nearly on the same straight line. However, one can still notice a small but definite trend for the composition dependence of both fitting parameters in the Arrhenius Eq. (1), $\tau_{\beta 0}$ and ΔE_β (Table IV). In fact, one observes a typical ''compensation effect'' consisting in an increase of ΔE_β concomitant with a decrease of $\log_{10}\tau_{\beta 0}$ with higher L/N ratio.

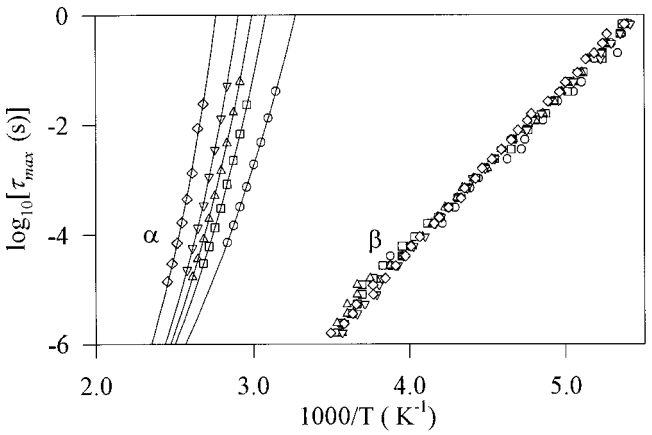

FIG. 4. Arrhenius plot of $\tau_{\max}$ as a function of reciprocal temperature. Symbols the same as in Fig. 2.

Judging by the unexpectedly low values of the preexponential factor ($10^{-17}<\tau_{\beta 0}<10^{-15}$ s), the β relaxations in the HPNs studied do not exactly fit Starkweather's definition [28] of ''simple'' relaxations with zero activation entropies (even though the values of ΔE_β do correlate with $T_{\max}$). Nevertheless, the small influence of the local environment, characterized by the network density, on the activation energies ΔE_β, combined with their fairly low absolute values (Table IV) are the typical features of a noncooperative relaxation in loosely packed regions of a glassy quasilattice.

B. Relaxation strength

As already mentioned above (see Fig. 1 and Tables II and III), both the intensity and dielectric strength of the β relaxations in HPNs increase with lower L/N ratio. This is in striking contrast to the case of the main α relaxation in polymer networks in general [29] and in HPNs in particular [24]. Here, the exactly opposite dependence was explained by steric constraints from network junctions on the segmental motion of network strands [24]. The same arguments were also invoked to explain the increase of T_g (or, equivalently, T_α) with increasing apparent network density as expressed through the L/N ratio.

TABLE IV. Activation energies and preexponential factors of the secondary relaxation.

L/N	ΔE_β (kJ mol^{-1})	$\tau_{\beta 0}$ (s)
100/0	54.0 ± 0.8	2.95×10^{-16}
75/25	55.3 ± 0.5	1.66×10^{-16}
60/40	55.2 ± 0.5	1.77×10^{-16}
43/57	57.4 ± 0.4	4.68×10^{-17}
0/100	58.3 ± 0.3	3.39×10^{-17}

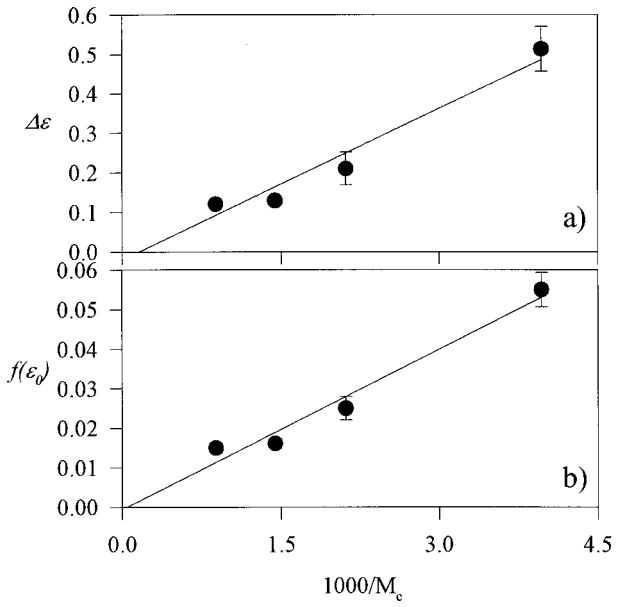

FIG. 5. Dielectric strength (a) and reduced dielectric strength (b) of the secondary relaxation as a function of $1/M_c$. Error bars take account of the temperature dependence of parameters.

It can be easily verified using the data from Table I that the kinetic free volume fractions at the respective T_g values calculated through the VTF equation (2) as [30]

$$f_g^K=(T_g-T_0)/B=[\ln(\tau_g/\tau_{a0})]^{-1} \tag{5}$$

are essentially composition invariant and close to the ''universal'' Williams-Landel-Ferry (WLF) value $f_g=0.025$ [31]. One can argue, however, that different patterns of free volume distribution may be possible for HPNs with the same average value of $\langle f_g^K\rangle$ frozen in at the corresponding T_g values. It seems reasonable to assume that the total free volume available will be distributed between the densely packed domains, characterized by a deficit of local free volume fraction compared to $\langle f_g^K\rangle$, and the remaining loosely packed matrix, where the local free volume fraction will be excess of $\langle f_g^K\rangle$. Taking into consideration that the inherent crystallizability of monomeric aliphatic isocyanurates [32,33] is lost once they are incorporated into the network, it is likely that the densely packed domains in the HPNs studied comprise linear, two-arm isocyanurate heterocycles (ISHs), while it is the loosely packed, three-arm ISHs that form the continuous, three-dimensional network structures. In terms of this model, the condition $\langle f_g^K\rangle=$const for all studied HPNs implies that the fraction of loosely packed network junctions will increase (i.e., the local free volume fraction in the densely packed domains will decrease with respect to $\langle f_g^K\rangle$) with increasing apparent network density. Thus, these qualitative considerations permit us to explain the observed composition dependence of the intensity of β relaxation by weaker interactions (couplings) in the network junction sites of HPNs with lower L/N ratios.

The same arguments may be invoked to explain the composition dependencies of the best-fit values of shape parameters in the HN equation (4) (cf. Fig. 3 and Table III), as well as of the dielectric strength and the fraction of active dipoles (Fig. 5) calculated by the Fröelich-Kirkwood equation (6) [34]:

$$f(\varepsilon_0)=\frac{(\varepsilon_0-\varepsilon_\infty)(2\varepsilon_0+\varepsilon_\infty)}{\varepsilon_0(\varepsilon_\infty+2)^2}=\frac{4\pi\rho N_a}{9kTM}g\mu^2, \tag{6}$$

where ρ is the density, μ is the dipole moment of the relaxing unit, M is the molecular weight of the repeating unit, g is the correlation factor, N_a is Avogadro's number, and k is the Boltzmann constant.

As can be seen from Fig. 5, both $\Delta\varepsilon$ and $f(\varepsilon_0)$ decrease linearly with increasing reciprocal apparent molar mass of chain strands between the network junctions, $\langle M_c\rangle$, down to $\Delta\varepsilon\approx 0$ for the linear structure at $\langle M_c\rangle\to\infty$. This result suggests that it is the effective network junctions formed by the three-arm ISHs and not the linear two-arm ISHs that make the major contribution to the β relaxation in HPNs at high network densities with low L/N ratios.

C. Mechanism of β-relaxation mobility

It seems pertinent to emphasize once again that all polar groups available in the HPNs studied are located in the ISHs; hence the same dipoles will be responsible for the dielectric response regardless of the relaxation mode. In this respect, these systems should be appropriate for testing the predictions of the coupling model (CM) [35,36].

The CM approach assumes the existence of a temperature-insensitive crossover time t_c separating the regime of faster (''primitive'') pure Debye-like mobility of kinetic units at $t<t_c$ where Eq. (1) holds from the regime of slower, constrained mobility at $t>t_c$ which sets in due to the increase of interactions (''couplings'') between kinetic units and is characterized by Eqs. (2) and (3). Thus, having identified the faster and the slower mobility regimes as the β and α relaxations, respectively, the condition of continuity of $\phi(t)$ at t_c implies the following relationship [37]:

$$\tau_\alpha(T_g)=[t_c(\beta_{\mathrm{KWW}}-1)\tau_0(T_g)]^{1/\beta}_{\mathrm{KWW}}. \tag{7}$$

According to Ngai's view, from a comparison of the experimental $\tau_\beta(T_g)$ values with those of $\tau_0(T_g)$ calculated from the previous equation assuming $t_c=2\times10^{-12}$ s and $\tau_\alpha(T_g)=10^2$ s, a linear relationship between $\tau_B(T_g)$ and β_{KWW} is expected [37]. The validity of the above relation can be tested in our case by considering a reference temperature T^* such that $\tau_\alpha(T^*)=10^2$ s and the β_{KWW} values previously reported (Table I). As can be seen from Fig. 6, our experimental data for τ_β at T^* are in reasonable agreement with the theoretical prediction as shown by the dashed line in Fig. 6 calculated with Eq. (7).

The correlation between the quantities characterizing β and α relaxations as expressed through Eq. (7) lends further support to the basic concept that there are identical kinetic units, either individual molecules for simple organic liquids or statistical chain segments for polymers, involved in both processes [38]. The major difference is in the mechanisms of their mobility, which should be noncooperative with low apparent activation energies for the β relaxation, and coopera-

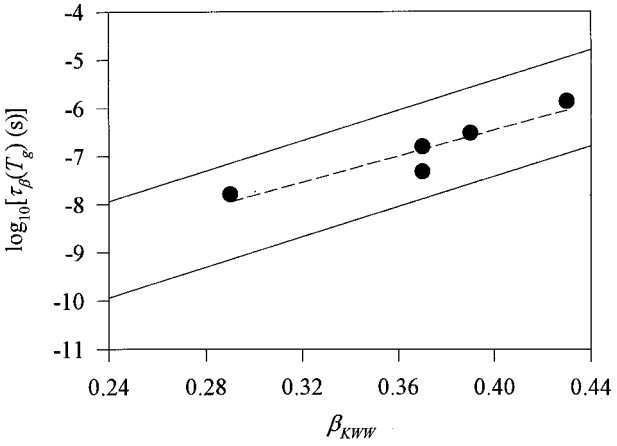

FIG. 6. $\log_{10}[\tau_\beta(T_g)]$ vs β_{KWW} plot. The solid lines were calculated from the coupling model, Eq. (7) [37] according to values of $\tau_\alpha(T_g)=10^4$ s (top line) and 10^2 s (bottom line). The dashed line represents the approximate straight line for experimental values.

tive with high apparent activation energies for the α relaxation. In both cases, the onset of mobility at each relaxation implies conformational rearrangements within the relevant kinetic units. It seems obvious that, in contrast to stiff aromatic heterocycles like cyanurates [23], the absence of conjugated bonds within ISHs makes the latter sufficiently flexible to allow for specific conformational transitions with deviation from the planar structure of the isocyanurate, like the ''chair-boat-chair'' transition in the structurally similar cyclohexyl ring [39]. The assumed similarity between conformational transitions in the cyclohexyl ring and in the ISH is qualitatively consistent with the proximities of their subglass relaxation temperatures (180–193 K at 1 Hz for the former [39], and 188–195 K for the latter). Additionally, the corresponding apparent activation energies (a slightly higher value for ISH of 50.4–58.3 kJ/mol, compared to the theoretical estimate of 45 kJ/mol for the cyclohexyl [39]) may be explained by the mobility constraints from couplings between the dipoles in neighboring ISHs and from the network architecture of the HPN system. More work is obviously needed to clarify this issue.

V. CONCLUSIONS

(1) The β relaxations in the HPNs investigated obey the Arrhenius law reasonably well with unusually low values of the preexponential factor of $10^{-17}<\tau_{\beta_0}<10^{-15}$ s. Nevertheless, the small influence of the local environment characterized by the network density on the apparent activation energies ΔE_β and their fairly low absolute values (50.4–58.3 kJ/mol) are the typical features of a noncooperative relaxation in loosely packed regions of a glassy quasilattice.

(2) Both the intensity and dielectric strength of β relaxations in HPNs increase with higher apparent network density (i.e., with lower L/N ratio). This effect is explained by the model assuming that the total, composition-invariant free volume available is distributed between densely packed domains comprising linear, two-arm isocyanurate heterocycles, and loosely packed, three-arm ISHs which form the continuous, three-dimensional network structures.

(3) The experimental data for HPNs confirms Ngai's correlation between the logarithm of the secondary β-relaxation time and the KWW stretching exponent for the primary α relaxation.

(4) It is suggested that the absence of conjugated bonds within isocyanurate heterocycles makes them sufficiently flexible to allow for specific conformational transitions with deviation from the planar structure of the isocyanurate, like the ''chair-boat-chair'' transition in the structurally similar cyclohexyl ring.

ACKNOWLEDGMENTS

V.Y.K. and V.P. thank Professor F. J. Baltá-Calleja for hospitality and encouragement at the Instituto de Estructura de la Materia, CSIC. The authors are indebted to MCYT (Grant No. FPA2000-0950), Spain, for generous support of this investigation.

[1] N. Saito, K. Okano, S. Iwayanagi, and T. Hideshima, in *Solid State Physics*, edited by F. Seitz and D. Turnbull (Academic, New York, 1963), Vol. 14, pp. 343–502.
[2] G. E. Roberts and E. F. T. White, in *The Physics of Glassy Polymers*, edited by R. N. Haward (Applied Science Publications, London, 1973), pp. 153–222.
[3] Y. Wada, in *Dielectric and Related Molecular Processes*, edited by M. Davies (The Chemical Society, London, 1977), Vol. 3, pp. 143–175.
[4] M. Goldstein, J. Chem. Phys. **51**, 3728 (1969).
[5] G. P. Johari and M. Goldstein, J. Chem. Phys. **53**, 1766 (1970); **53**, 2372 (1970).
[6] G. P. Johari, J. Chem. Phys. **58**, 1766 (1973).
[7] H. Fujimori and M. Oguni, Solid State Commun. **94**, 157 (1995).
[8] J. Perez, J. Y. Cavaille, and V. P. Privalko, J. Non-Cryst. Solids **172**, 1028 (1994).
[9] A. Arbe, D. Richert, J. Colmenero, and B. Farago, Phys. Rev. E **54**, 3853 (1996).
[10] F. H. Stillinger, J. Chem. Phys. **89**, 6461 (1988).
[11] Y. N. Huang, Y. N. Wang, and E. Riande, J. Chem. Phys. **111**, 8503 (1999).
[12] F. Garwe, A. Schönhals, H. Lockwenz, M. Beiner, K. Schröter, and E. Donth, Macromolecules **29**, 247 (1996).
[13] C. A. Angell, Science **267**, 1924 (1995).
[14] M. B. M. Mangion and G. P. Johari, J. Polym. Sci., Part B: Polym. Phys. **28**, 71 (1990).
[15] D. Sidebottom and G. P. Johari, Chem. Phys. **147**, 205 (1990).
[16] M. B. M. Mangion and G. P. Johari, J. Polym. Sci., Part B: Polym. Phys. **29**, 437 (1991).
[17] M. G. Parthun and G. P. Johari, J. Chem. Phys. **103**, 7611 (1995).
[18] D. A. Wasylyshyn and G. P. Johari, J. Chem. Phys. **104**, 5683 (1996).

[19] G. P. Johari and W. Pascheto, J. Chem. Soc., Faraday Trans. **91**, 343 (1995).
[20] G. P. Johari, J. Chem. Soc., Faraday Trans. **93**, 2303 (1997).
[21] A. Schönhals and E. Schlosser, Colloid Polym. Sci. **267**, 133 (1989).
[22] A. R. Kannurpatti and C. N. Bowman, Macromolecules **31**, 3311 (1998).
[23] B. D. Fitz and J. Mijovic, Macromolecules **32**, 3518 (1999).
[24] V. Yu. Kramarenko, T. A. Ezquerra, I. Sics, F. J. Balta-Calleja, and V. P. Privalko, J. Chem. Phys. **113**, 447 (2000).
[25] K. L. Ngai and C. M. Roland, Macromolecules **27**, 2454 (1994).
[26] K. L. Ngai, C. M. Roland, and A. F. Yee, Rubber Chem. Technol. **66**, 817 (1993).
[27] S. Havriliak and S. Negami, Polymer **8**, 161 (1967).
[28] H. W. Starkweather, Macromolecules **14**, 1277 (1981).
[29] C. M. Roland, Macromolecules **27**, 4242 (1994).
[30] V. P. Privalko, J. Non-Cryst. Solids **255**, 259 (1999).
[31] J. D. Ferry, *Viscoelastic Properties of Polymers* (Wiley, New York, 1970).
[32] K. Fukui, F. Tanimoto, and H. Kitano, Bull. Chem. Soc. Jpn. **38**, 1586 (1965).
[33] C. Shimasaki, H. Nakayama, A. Iwaki, E. Tsukurimishi, T. Yoshimura, and K. Hasegawa, Bull. Chem. Soc. Jpn. **65**, 1993 (1992).
[34] P. Hedvig, *Dielectric Spectroscopy of Polymers* (Hilger, Bristol, 1977).
[35] K. Y. Tsang and K. L. Ngai, Phys. Rev. E **54**, 3067 (1997).
[36] K. L. Ngai and K. Y. Tsang, Phys. Rev. E **60**, 4511 (1999).
[37] K. L. Ngai, Phys. Rev. E **57**, 7346 (1998).
[38] V. A. Bershtein and V. M. Egorov, *Differential Scanning Calorimetry in the Physical Chemistry of Polymers* (Khimia, Leningrad, 1990) (in Russian).
[39] J. M. G. Cowie, J. Macromol. Sci., Phys. **B18**, 569 (1980).